13th Int. Symp. on Applications of Laser Techniques to Fluid Mechanics
Lisbon, Portugal, 26–29 June, 2006
Paper #1091

2D3C-Laser Doppler Sensor for highly spatially resolved flow field investigations

Lars Büttner, Christian Bayer, Katsuaki Shirai, Andreas Voigt, Jürgen Czarske

Dresden University of Technology, Professorship for Measuring and Testing Techniques
Helmholtzstraße 18, D-01069 Dresden, Germany
Internet: http://eeemp1.et.tu-dresden.de, E-Mail: Lars.Buettner@tu-dresden.de

Abstract We report about a novel laser Doppler field sensor, which is capable of measuring the three-component (3C) velocity field in fluid flows in a two-dimensional area (2D) without mechanical scanning and without using a camera. The sensor is based on laser Doppler velocimetry but employs four superposed fan-like interference fringe systems. A spatial resolution in the sub-micrometer range can be achieved enabling highly spatially resolved flow studies. Possible applications are investigations in micro-fluidics, turbulence studies or precision flux measurements.

1. Introduction

For non-invasive investigations of flow fields numerous optical measurement techniques are available. Camera-based techniques like Particle Image Velocimetry (PIV), which is a well established method, and recently Doppler Global Velocimetry (DGV) are able to capture the velocity distribution inside a two-dimensional laser light sheet.
Especially in the field of micro-fluidics, where flows through channels of only a few 100 microns linear dimension are of interest, special effort is needed when imaging techniques like PIV are to be applied. At µ-PIV the flow is observed through a microscope objective [2]. Consequently only short working distances can be achieved and the depth resolution is determined by the depth of focus, whereas the lateral resolution is limited by diffraction and the pixel resolution of the camera. PIV exhibits an uncertainty of the velocity in the range of a few percent.
Doppler Global Velocimetry (DGV) uses a spectroscopic evaluation of the Doppler shift by means of an absorption cell. The experimental effort is significantly higher than that of PIV and the uncertainty of the velocity is usually around 1 m/s.
On the other hand, laser Doppler velocimetry (LDV) [1] is a well established method for point-wise measurements and offers a significantly higher accuracy of the velocity than camera-based methods. LDV utilizes an interference pattern of nearly parallel fringes generated in the volume of intersection of two crossing coherent laser beams. Tracer particles carried by the flow scatter light which is amplitude modulated with the Doppler frequency f. The velocity can be determined by $v = f\,d$, where d is the spacing of the interference fringes. The achievable precision of the velocity measurement is typically in the range of 1% ... 0.1% and is therefore considerably better than that of PIV or DGV. LDV is, however, a point-wise method so that for the investigations of fluid flow fields mechanical traversing is necessary, which is time consuming and needs additional experimental effort.
In this paper we report on an extended LDV for flow imaging which combines the strengths of LDV and µ-PIV. It is capable of measuring the three component velocity vector in a flow field with high precision without the use of a camera and without mechanical traversing. It is based on two orthogonally aligned velocity line sensors, each of which can measure the lateral velocity component, the axial velocity component and the axial position with respect to its optical axis.

2. The Laser Doppler Velocity Line Sensor

The laser-Doppler velocity line sensor [3-6] works by superposing two fan-like interference fringe systems which have to be physically distuinguishable (e.g. by carrier frequency multiplexing or wavelength multiplexing), one with convergent, the other with divergent fringes, see fig. (1).

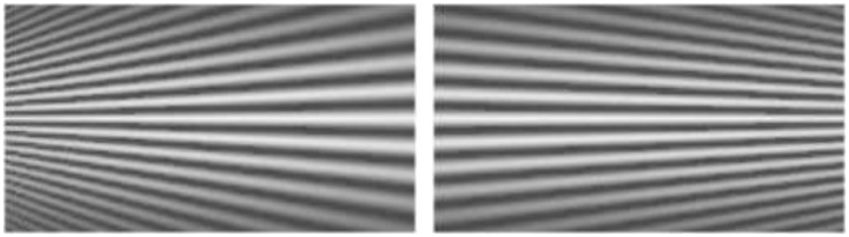

Fig. (1): Superposed fan-like interference fringe systems of the laser-Doppler line sensor

In order to generate the convergent and divergent fringes, the beam waists of the Gaussian laser beam have to be placed behind and before the crossing point of the LDA partial beams [7]. These distorted fringe systems are a consequence of the wavefront-curvature of the Gaussian laser beams.

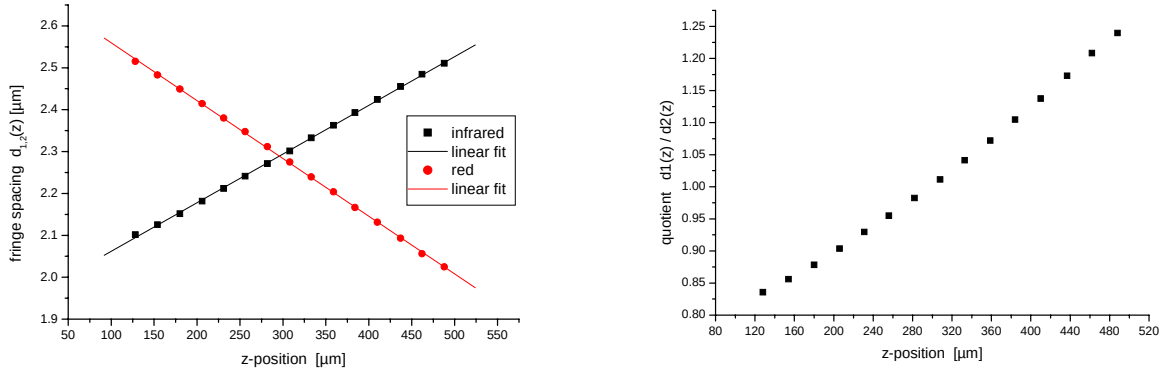

a) **b)**

Fig. (2): a) Increasing and decreasing fringe spacings $d_{1,2}(z)$ of the two superposed interference fringe systems as a function of the axial position. b) Quotient of the fringe spacings $q(z)=d_1(z)/d_2(z)$.

Fig. (2)a) shows the fringe spacing $d_{1,2}(z)$ as a function of the position along the optical axis z and fig. (2)b) the calculated calibration function, i.e. the quotient $q(z)=d_1(z)/d_2(z)$.
If a scattering particle, that is carried with the flow, passes the measurement volume perpendicularly to the optical axis it generates two burst signals, one from each fringe system. Doppler frequencies $f_{1,2}$ are now obtained from both of the fringe systems. If the quotient of the Doppler frequencies is considered,

$$q(z) = \frac{f_2(v_x, z)}{f_1(v_x, z)} = \frac{v_x / d_2(z)}{v_x / d_1(z)} = \frac{d_1(z)}{d_2(z)}$$

it becomes obvious that it is independent of the velocity v_x and depends only on the position z along the opical axis. The quotient of the Doppler frequencies can therefore be used to determine the axial position z. Fig. (2)b) shows the monotonic quotient function, calculated from the fringe spacing curves of fig. (2)a). The velocity of the tracer particle can be calculated by the Doppler frequencies and the local fringe spacing values at the known position z:

$$v_x(z) = f_1(v_x, z)\, d_1(z) = f_2(v_x, z)\, d_2(z)$$

In contrast to conventional LDV the axial position of the tracer particle inside the measurement volume can be determined additionally. Therefore the laser Doppler line sensor offers a significantly higher resolution than conventional LDVs [3,4].

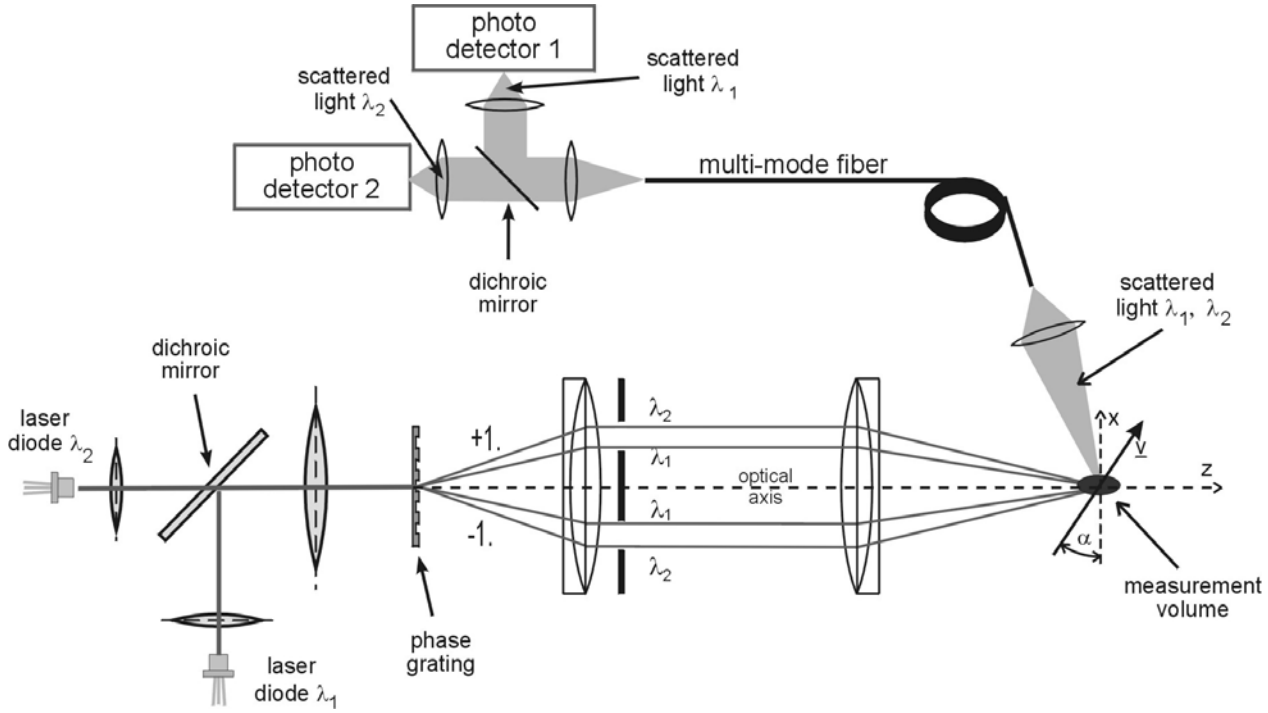

Fig. (3): Experimental setup of the laser Doppler line sensor.

Fig. (3) shows the experimental realization of the sensor principle. The beams of two laser diodes of different wavelengths (red: 660 nm and infrared: 785 nm) were collimated by aspheric lenses, collinearly superposed by a dichroic mirror and focused onto a diffraction grating. The ±1st diffraction orders were used as the LDA-partial beams, other diffraction orders were blocked by beam stops. A Keplerian telescope collimated the partial beams and made them intersect again. The four beams (two partial beams for each wavelength) intersected at one position so that two superposed interference fringe systems were generated. In order to obtain fan-like fringe systems (infrared: divergent fringes, red: convergent fringes) the beam waists of the Gaussian beams have to be place before or behind the common crossing point, respectively. This was achieved by adjusting the laser diode collimating lenses individually. The scattered light from the tracer particles was coupled by a single lens into a multimode fiber and guided to a detection unit. Here the light was split by a dichroic mirror into the different wavelengths and each wavelength was detected by a single avalanche photo detector. The photo detector signals were acquired by a standard PC with a 12-Bit analogue/digital converter card. A LabVIEW program was used to process the data.

For adjustment, characterisation and test of the sensor a thin wire acted as a scattering particle. It was fixed at an optical chopper, which rotated at stabilized angular velocity, providing a velocity reference.

Test measurements revealed a spatial resolution in the submicrometer-range and an uncertainty of the velocity $<5 \cdot 10^{-4}$ [3].

In contrast to conventional LDV the mechanical scanning of the pointwise measurement volume can now be omitted and velocity profiles can be measured as a whole. The size of the measurement volume of the LDA line sensor can be adapted to the region of interest of the flow and velocity profiles can be measured without mechanical traversing of the sensor head.
The sensor was successfully applied to highly spatially resolved measurements of laminar [3] and turbulent [5] boundary layer flows.

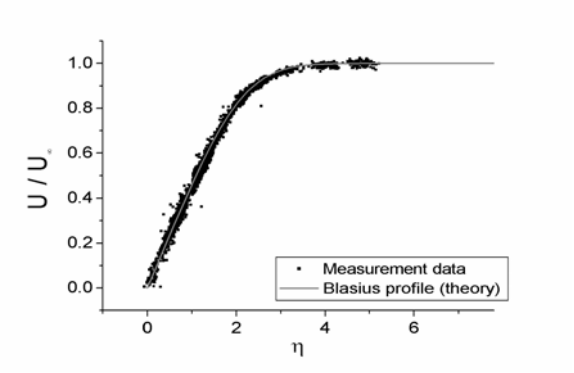

Fig. (4): Measured linear velocity profile of a laminar flat-plate boundary layer flow (normalized coordinates).

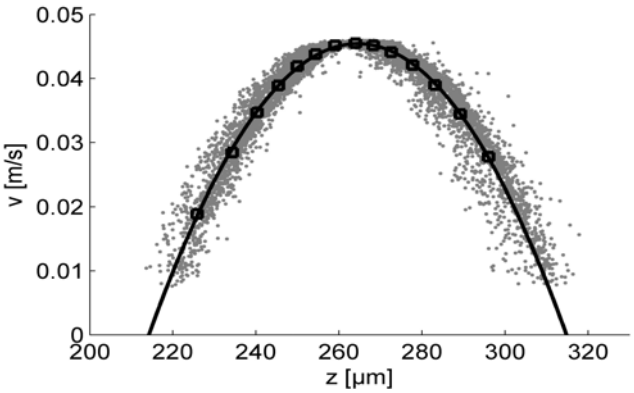

Fig. (5): Measured velocity profile inside a micro-channel of 100 µm width (solid line: fitted parabolic curve).

Fig. (4) shows the velocity profile of a laminar boundary flow around a flat plate (Blasius profile) measured with the laser Doppler line sensor. Each data point in the plot represents one single tracer particle, whose position and velocity were determined. Since the tracer particles are distributed statistically over the flow, the entire velocity profile can be recovered by evaluating a sufficient number of tracer particles. The measured profile agrees perfectly with the Blasius function (solid curve).

Another possible application field of the profile sensor is micro-fluidics. Fig. (5) shows the measured velocity profile along the short axis of a rectangular micro-channel of 100 µm x 2000 µm cross-section. Distilled water seeded with polystyrene particles of 2 µm diameter was used as a working fluid. The channel flow was driven by hydrostatic pressure. The solid curve shows a parabolic fit of the measurement data. The theoretical expected parabolic profile is in excellent agreement with the measurement data. The channel width estimated from the fit at the velocity profile is 101.5 µm and agrees also well with the true channel dimension. From the scattering of the measured data the spatial resolution was estimated to ±3.5 µm.
This experiment clearly demonstrates the suitability for flow measurement with micrometer spatial resolution.

3. Determination of the Axial Velocity Component by Chirp Detection

The sensor principle can be extended to measure also the axial velocity component v_z. For the generalized case of inclined trajectories, i.e. for a significant axial velocity component the Doppler frequency of the burst signal will not be constant but will vary with time [6] since the fringe spacing varies with the axial position.
Fig. (6) shows the coordinate system and the parameters of the tracer particle movement for the more generalized case that the velocity vector has a finite axial component. The x- and z- velocity component are then linked to the angle α between the particle trajectory and the optical axis by:

$$v_x = v\cos\alpha \quad , \quad v_z = v\sin\alpha \quad , \quad \tan\alpha = \frac{v_z}{v_x}$$

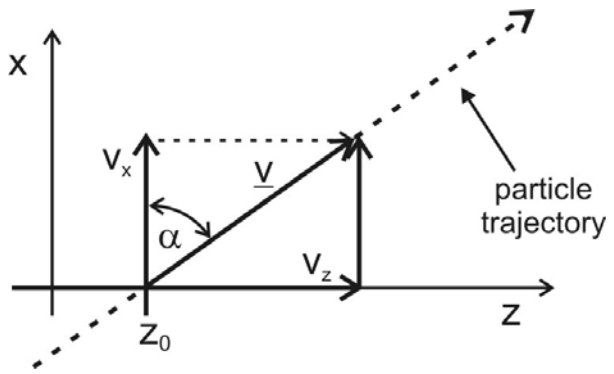

Fig. (6): Coordinate system and parameters of the tracer particle movement in the case of tilted trajectories.

The fringe spacing functions $d_{1,2}(z)$ are assumed to vary linearly with the axial position z, which is fulfilled in a very good approximation, see fig. (2)a):

$$d_1(z) = d_{01} + c_1 \cdot z$$
$$d_2(z) = d_{02} + c_2 \cdot z$$

The particle trajectory can then be written by means of the time-dependent x-coordinate $x(t)=v_x \cdot t$ and z-coordinate $z(t)=v_z \cdot t+z_0$, where z_0 denotes the z-position for the time t=0, which in the following will be referred to as the "offset-position". This will be the axial position at which the particle passed the optical axis. By substituting these expressions and the fringe spacing functions $d_{1,2}(z)$ into the general expression for the Doppler frequency $f=v_x/d$ we obtain the time dependent Doppler-frequency:

$$f_{1,2}(v_x, v_z, z_0, t) = \frac{v_x}{d_{1,2}(z(t))} = \frac{v_x}{d_{01,2} + c_{1,2} v_z t + c_{1,2} z_0}$$

Obviously, with non-vanishing axial velocity component v_z the frequency of the burst signal is no longer constant but varies with time (chirp-signal). Since the signs of the $c_{1,2}$ coefficients are opposite, the burst signal of one fringe system will exhibit an "up-chirp", and the burst signal from the other fringe system a "down-chirp". The frequency funtions are, however, hyperbolically varying. In contrast, the period time – time functions $T_{1,2}(t)= f_{1,2}(t)^{-1}$ will exhibit a linear relationship.
If the equation is differentiated with respect to time all constant addends vanish and a time-independent constant results as the derivative:

$$\frac{dT_{1,2}(t)}{dt} = c_{1,2}\frac{v_z}{v_x}$$

Obviously, the chirp can be used to directly measure the axial velocity component. From the preceding derivation it is evident that the method has the following properties:

- There is a direct, linear relationship between the change of the period time and the v_z-component.

- The strength of the chirp depends also on the v_x-component which means that the v_z-component can only be measured relative to the v_x-component. More precisely, the chirp is a measure for the ratio of or angle between both velocity components.
- The axial velocity component is directional discriminating. Usually, the lateral velocity component v_x has an ambiguity with respect to the direction, since only a positive frequency can be measured, so that a directional discrimination is not possible. To achieve a directional discrimination, additional frequency-shift-elements like AOMs have to be included, which introduce a carrier frequency onto the Doppler signal. In contrast, the chirp $dT_{1,2}(t)/dt$ can be both positive and negative, so that the determination of the axial component v_z is a priori sensitive to the direction of the particle movement. No additional frequency shift elements or other extensions of the set-up are needed.
- From one single tracer particle the following variables of its trajectory can be determined:
  - the lateral velocity component v_x
  - the axial velocity component v_z including its sign (direction)
  - the position z_0 of the passage through the optical axis ("offset-position")

For the determination of the axial velocity component no modification of the sensor setup in necessary, just the signal processing has to be extended by a chirp detection algorithm. It is based on a Short-Time Fast-Fourier-Transform (ST-FFT, or sliding FFT). At first, the envelopes of the burst signals are calculated by means of a Hilbert transform. The point of time with maximum amplitude is detected, indicating the time when the particle passed the optical axis, where the maximum intensity occurs. Then the signals were truncated to their $1/e^2$-borders und normalized. The ST-FFT was used to calculate the Doppler-frequency-time functions, which, after calculating their reciprocals, yielded the period time – time functions. The period time-time functions were fitted by linear regressions. From the regression parameters the frequencies at the time t_{Max}, where the maximum amplitudes occur, are calculated. These frequencies represent the momentary frequencies for that point of time, at which the particle passed the optical axis and are therefore used for the determination of the offset-position z_0 and the transverse velocity component v_x. From the slope of the linear regression curves and the v_x-component the axial velocity component v_z are derived. Fig. (7)a) shows as an example the chirped burst signal pair of a particle, which passed under an angle of α=30° through the measurement volume.

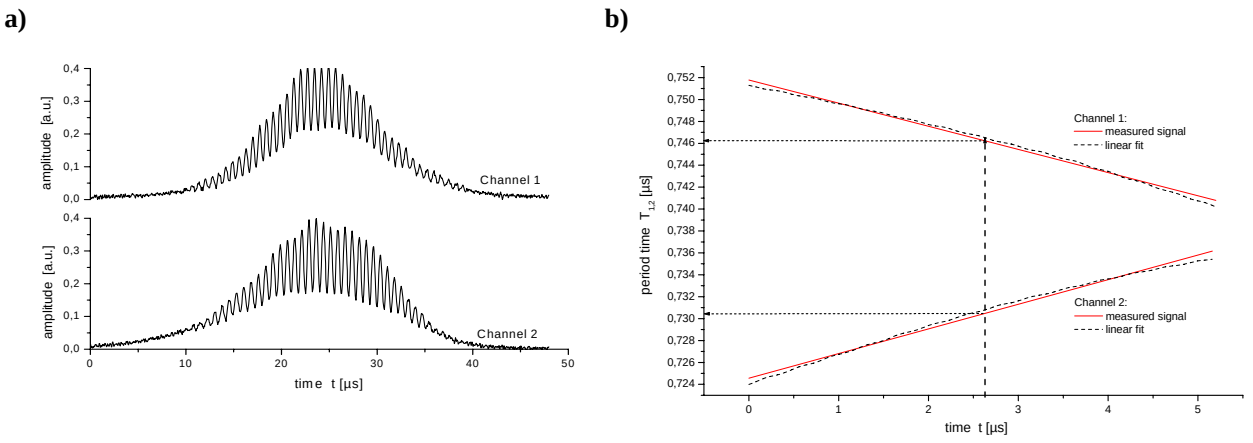

Fig. (7): a) Chirped burst signal pair from a particle passing with α=30° to the optical axis. b) Period time – time functions for both channels, obtained from the short-time FFT. The momentary values at the marked point of time are used to calculate the offset position z_0 and the lateral velocity component v_x, whereas the slope of the functions yields the axial v_z-component.

Fig. (7)b) shows the resulting period time – time functions [6] including their linear regression curves (solid curves) for a particle passing under an angle of α=30° through the measurement volume. The dashed line indicates the point of time, at which the particle passed trough the optical axis. From the momentary frequencies at this point of time the lateral velocity component v_x and the offset position z_0 are calculated, whereas the axial velocity component is derived from the slope of the linear regression curves.

a) **b)**

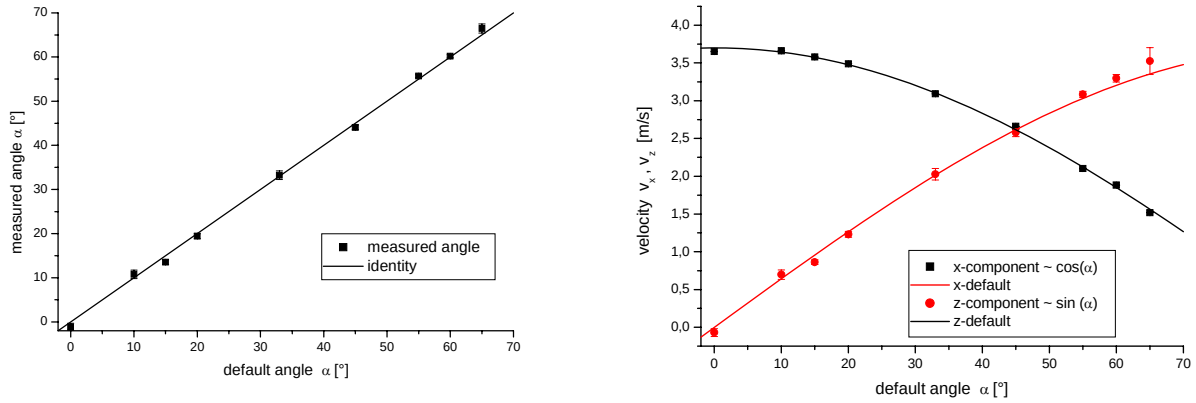

Fig. (8): Test of a) the angle and b) the velocity component measurement for different inclination angles of an calibration object. An excellent agreement between the default and the measured values occurs.

Fig. (8a,b) show a measurement with a calibration object, which was aligned at different angles α with respect to the optical axis of the sensor. The measured angle agrees well with the installed angle (default), see fig. (8)a). Fig (8)b) shows the measured velocity components, which behave like sinα and cosα functions. The experiments revealed an uncertainty of 3% for the axial velocity component, an uncertainty of the flow angle α of 0.7° (angle between the axial and lateral velocity component) und a spatial resolution of the offset position z_0 of 1.5 µm at a signal-to-noise-ratio (SNR) of the burst signals of 20 dB [6].

a) **b)**

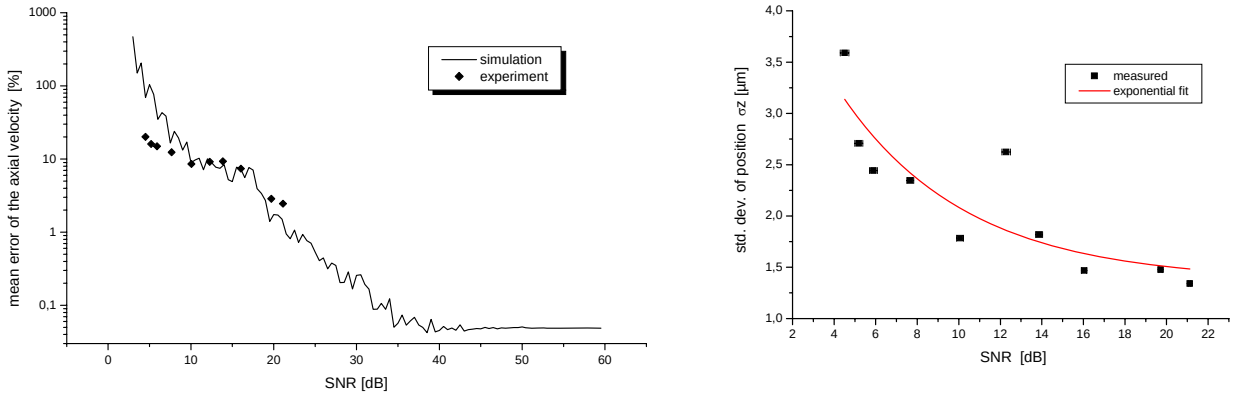

Fig. (9): Uncertainty estimation of a) the axial velocity component v_x (solid: simulation, dotted: experiment) and b) of the offset position z_0 (dotted: measurement, solid: exponential fit) in dependence from the SNR.

Fig. (9) shows estimations of the measurement uncertainty for the axial velocity component v_x and the offset position z_0 for different SNRs. The measurement uncertainty is exponentially decreasing with rising SNR.

With the laser Doppler line sensor with implemented chirp-detection it is therefore possible to determine

- the lateral velocity component
- the axial velocity component
- the axial position inside the measurement volume

of one single tracer particle.

4. Combination of 2 Line Sensors with Chirp Detection to the 2D3C Laser Doppler Field Sensor

The laser Doppler velocity line sensor described above measures the (1D) velocity profile along one line. In order to achieve velocity measurements not only in a line but in a two-dimensional area two line sensors can be combined orthogonally such that their measurement volumes overlap. Each of the line sensors can measure one component of the two-component position vector inside the plane which is spanned by the line sensors. Tab. (1) gives an overview of the quantities which can be measured when the two line sensors are oriented along the x- and y-direction.

	line sensor 1	line sensor 2
direction of optical axis	y	x
lateral component	v_z	v_z
axial component	v_y	v_x
position coordinate	y	x

Tab. (1): Combination of two line sensors to a 2D3C field sensor

Note that the coordinate system is now different to one used before and now refers to fig. (9). The axial velocity component of each line sensor is obtained by means of chirp detection.
Obviously it is possible to determine all three velocity components and the two-dimensional position inside the volume of intersection, i.e. the size:

$$\vec{v}(x,y) = \begin{pmatrix} v_x(x,y) \\ v_y(x,y) \\ v_z(x,y) \end{pmatrix}$$

can be determined for a single tracer particle. By evaluating a sufficient number of tracer particles the entire three-component (3C) velocity distribution can be reconstructed in the two-dimensional (2D) plane of observation without mechanical traversing, see fig. (9). Even though no camera is needed, an image of the velocity distribution of the flow field can be measured.

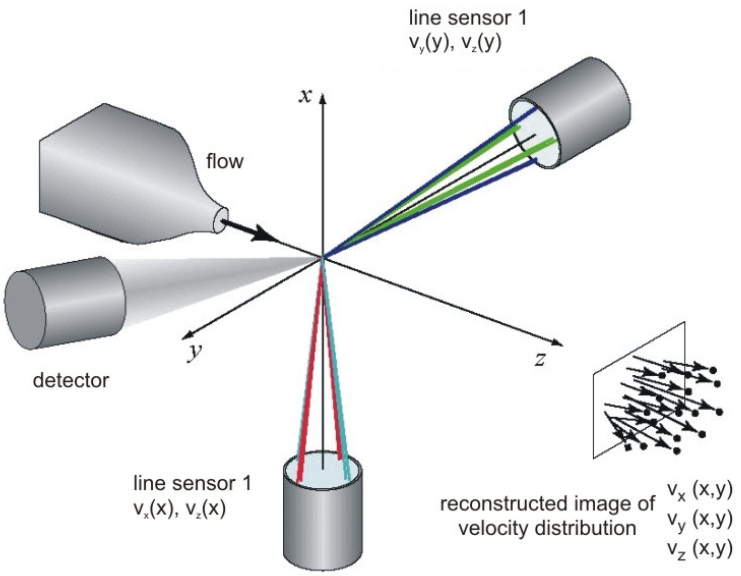

Fig. (9): Concept of the 2D3C-laser Doppler field sensor

The four interference fringe systems have to be physically distinguishable which can be achieved by wavelength division multiplexing (WDM) [4], carrier frequency division multiplexing (FDM) [5] or combinations of it. The number of single photo detectors needed depends of the realization of multiplexing and can range from one (if pure FDM is used) to four (if pure WDM is used). In all cases just one detection unit is necessary consisting of a single lens to couple the light into one multimode-fiber, see fig. (3).

This sensor concept, presented here for the first time, offers several advantages compared to PIV:

- Since the sensor principle is based on LDA, only a single detection unit consisting of a single lens to couple the light into a multimode fiber is needed. An image of the velocity distribution of a flow field can be achieved without using a camera.
- Since the sensor is based on the difference Doppler technique, the signals will not depend on the observation vector. Consequently, the detector can be located arbitrarily around the measurement volume. In particular, detection can be realized in backward scattering arrangement, so that the detection unit can be integrated collinear in the sending optics and no additional optical access is required.
- At µ-PIV the longitudinal resolution is limited by the depth of focus, which is usually several micrometers. The lateral resolution usually does not subside 1 µm, even when sub-pixel interpolation is used. In contrast, the laser Doppler field sensor offers a higher spatial resolution down to the sub-micrometer range [4].
- µ-PIV offers only very short working distances (spacing between the sensor and the measurement volume) of a few millimetres due to the short focal length of the employed microscope objectives. In contrast, the working distance of the laser Doppler field sensor can be several centimetres [4].

5. Summary

We presented for the first time an extended laser Doppler velocimetry (LDV) sensor which is capable to measure the distribution of the three component velocity vector inside a two-dimensional area, i.e. the quantity

$$\vec{v}(x,y) = \begin{pmatrix} v_x(x,y) \\ v_y(x,y) \\ v_z(x,y) \end{pmatrix}$$

for a single tracer particle passing the measurement volume. It is based on two orthogonally aligned line sensors each of which can measure the lateral velocity component, the axial velocity component and an axial position with respect to its optical axis. The measurement volume of one line sensor consists of two superposed fan-like interference fringe systems which have to be physically distinguishable. An uncertainty of $<5\cdot10^{-4}$ for the lateral velocity component, 3% for the axial velocity component (corresponding to an uncertainty of the flow angle of <3°) and a spatial resolution of <1 µm can be achieved. The line sensor was successfully applied for measuring laminar and turbulent boundary layer flow and also for measuring the velocity profile inside a 100 µm wide micro-channel with micrometer spatial resolution.
The 2D3C laser Doppler field sensor will be able to measure an image of the velocity distribution inside a two-dimensional area without using a camera. Because of its high spatial resolution it is superior to standard laser Doppler anemometry and even to µ-PIV.
Possible applications range from micro-fluidics (investigation of micro- fluidic devices like micro-mixers, etc.) over fundamental turbulence research (investigations of small eddies down to the Kolmogorov scale) to precise flux measurements.

Acknowledgement
The authors thank H. Höhne for developing the water calibration rig and D. Petrak for providing the micro-channel equipment. The funding by the Deutsche Forschungsgemeinschaft (funding code Cz55/18-1 within the priority program SPP1147) is greatly acknowledged.

References

[1] H. Albrecht, M. Borys, N. Damaschke, C. Tropea, “Laser-Doppler and phase-Doppler measurement techniques“, Heidelberg: Springer, 2002
[2] J.G. Santiago, S.T. Wereley, C. Meinhart, B.J. Beebee, and R.J. Adrian, “A PIV system for microfluidics”, Exp. Fluids, Vol 25, No. 4 pp. 316-319 - 1998
[3] J. Czarske, L. Büttner, T. Razik, H. Müller, „Boundary layer velocity measurements by a laser Doppler profile sensor with micrometre spatial resolution”, Meas. Sci. Technol. 13, pp. 1979-1989, 2002
[4] L. Büttner, J. Czarske, H. Knuppertz, „Laser Doppler velocity profile sensor with sub-micrometer spatial resolution employing fiber-optics and a diffractive lens“, Applied Optics 44, No. 12, pp. 2274-2280, 2005
[5] K. Shirai, T. Pfister, L. Büttner, J. Czarske, H. Müller, S. Becker, H. Lienhart, F. Durst, “Highly Spatially Resolved Velocity Measurements of a Turbulent Channel Flow by a Fiber-Optic Heterodyne laser-Doppler Velocity-Profile-Sensor“, Exp. Fluids 40, Nr. 3, S. 473-481, 2006
[6] L. Büttner, J. Czarske, “Determination of the axial velocity component by a laser Doppler velocity profile sensor”, J. Opt. Soc. Am. A, Vol. 23, pp. 444-454, 2006
[7] Paul C. Miles, “Geometry of the fringe field formed in the intersection of two Gaussian beams”, Appl. Opt. 35, No. 30, pp. 5887-5895, 1996